

Mitochondrial frataxin interacts with ISD11 of the NFS1/ISCU complex and multiple mitochondrial chaperones

Yuxi Shan, Eleonora Napoli and Gino Cortopassi*

VM:Molecular Biosciences, 1311 Haring Hall, Davis, CA, 95616, USA

Received January 23, 2007; Revised and accepted February 19, 2007

The neurodegenerative disorder Friedreich's ataxia (FRDA) is caused by mutations in frataxin, a mitochondrial protein whose function remains controversial. Using co-immunoprecipitation and mass spectrometry we identified multiple interactors of mitochondrial frataxin in mammalian cells. One interactor was mortalin/GRP75, a homolog of the yeast *ssq1* chaperone that integrates iron–sulfur clusters into imported mitochondrial proteins. Another interactor was ISD11, recently identified as a component of the eukaryotic complex Nfs1/ISCU, an essential component of iron–sulfur cluster biogenesis. Interactions between frataxin and ISD11, and frataxin and GRP75 were confirmed by co-immunoprecipitation experiments in both directions. Immunofluorescence analysis demonstrated that ISD11 co-localized with both frataxin and with mitochondria. The point mutations I154F and W155R in frataxin cause FRDA and are clustered to one surface of the protein, and these mutations decrease the interaction of frataxin with ISD11. The frataxin/ISD11 interaction was also decreased by the chelator EDTA, and was increased by supplementation with nickel but not other metal ions. Nickel supplementation rescued the defective interaction of mutant frataxin I154F and W155R with ISD11. Upon ISD11 depletion by siRNA in HEK293T cells, the amount of the Nfs1/ISCU protein complex declined, as did the activity of the iron–sulfur cluster enzyme aconitase, while the cellular iron content was increased, as seen in tissues from FRDA patients. Furthermore, ISD11 mRNA levels were decreased in FRDA patient cells. These data suggest that frataxin binds the iron–sulfur biogenesis Nfs1/ISCU complex through ISD11, that the interaction is nickel-dependent, and that multiple consequences of frataxin deficiency are duplicated by ISD11 deficiency.

INTRODUCTION

Friedreich's ataxia (FRDA) is the most common autosomal recessively ataxia, with an incidence of ~1:50 000 (1). Like the autosomal dominant spinocerebellar ataxias, the major clinical sign of the disease is loss of coordination and unsteadiness of gait. However, hypertrophic cardiomyopathy and insulin resistance are also common in FRDA (1–3).

FRDA is usually caused by inheritance of two expanded alleles of (GAA)*n* triplet repeat in the first intron of frataxin gene (4). Expansions are thought either to partially inhibit transcription elongation (5), or to condense chromatin structure (6,7) and thus reduce frataxin protein expression (8). Both the severity of the FRDA and the age of onset are directly related to size of the smaller GAA expansion (9).

Frataxin is thought to support the biogenesis of iron–sulfur clusters, since its deficiency specifically affects iron–sulfur cluster enzymes (10) and because it interacts with ISCU, which is thought to be the main scaffold on which iron–sulfur clusters are built (11–14). Recent *in vitro* studies proved that frataxin interacts with the iron–sulfur cluster containing enzymes mitochondrial aconitase (15) and ferredoxin (an ISC protein in mammals) (16–18), while in yeast and *Caenorhabditis elegans* it interacts with succinate dehydrogenase (19,20). Knockdown of the frataxin message causes a decrease in the maturation of iron–sulfur cluster proteins (21–23). Microarray analysis of human cells has shown that frataxin depletion affects iron–sulfur cluster-related transcripts preferentially (24).

To identify frataxin's interactors, we carried out co-immunoprecipitation, electrophoresis, band cutting and

*To whom correspondence should be addressed at: Tel: +1 5307549665; Fax: +1 5307549342; Email: gcortopassi@ucdavis.edu

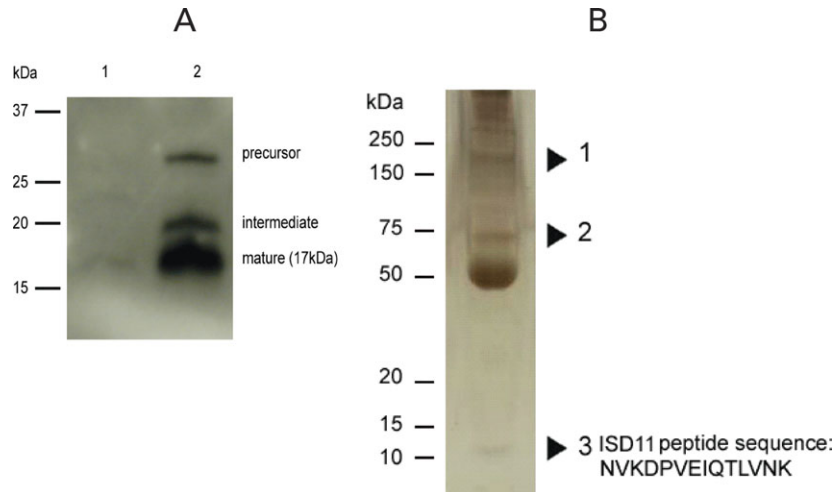


Figure 1. Immunoaffinity purification of human frataxin. (A) mitochondrial lysates of COS7 cells were analyzed with anti-frataxin antibody. Lane 1, untransfected cells; lane 2, cells transfected with pcDNA3.1-frataxin-flag plasmids. (B) Silver staining of affinity-purified frataxin complexes from mitochondrial extract of transfected COS7 cells. Bands were cut and analyzed by mass spectrometry, and the ISD11 peptide sequence is presented.

Table 1. Mitochondrial proteins associated with human frataxin

Sequence coverage (%)	Protein identified	Abbreviation	Peptides matched		Total	MW	Accession #
			COS7	Lympho			
28	Mortalin, GRP75, hsp70 9B	HSPA9B/GRP75	11	1	12	73.6	24234688
14	isd11/chromosome 6 orf 149	C6orf149/ISD11	1	—	1	10.8	38570053
11	ATP synthase, F0 subunit G	ATP5L	1	—	1	11.4	51479156
9	hsp 60, GroEL, SPG13	HSPD1	4	1	5	61.2	77702086
7	ATPase family, AAA domain	ATAD3A	3	—	3	72.5	42476028
7	Frataxin isoform 1 preproprotein	FRATAXIN	1	—	1	23.1	31077081
2	Succinate dehydrogenase A	SDHA	1	1	1	70.9	4759808
1	AFG3 ATPase family gene 3-like 2	AFG3L1	1	—	1	88.5	5802970

Caption. COS7 = COS7 cells, Lymph = lymphotolasts, mul = molecular weight.

mass spectrometric identification. We isolated GRP75, an ssq1 homolog and ISD11, a recently identified component of the Nfs1/ISCU scaffold complex (25,26), and confirmed their interaction with frataxin by multiple means, i.e. co-immunoprecipitation in both directions, GST-pulldown, and colocalization. Here we show that frataxin interacts with ISD11 in a mutation-dependent and nickel-dependent fashion, and that knockdown of ISD11 phenocopies two consequences of frataxin inhibition, namely aconitase deficiency and cellular iron overload.

RESULTS

Frataxin associates with multiple mitochondrial proteins

We searched for novel interaction partners of frataxin in two ways. One method included the preparation of protein extracts from lymphoblast mitochondria, followed by immunoprecipitation with anti-frataxin antibody, separation of proteins via electrophoresis, band isolation, digestion and mass spectrometry. However, the efficiency of the process was further enhanced by overexpressing frataxin. So, a vector (pcDNA3.1-frataxin-flag) was constructed which expressed frataxin protein with a

C-terminal flag epitope tag. This construct drove high frataxin expression in COS7 cells as detected by anti-frataxin antibody, and maximal amount of mature mitochondrial frataxin was produced at post-transfection day 5 (Fig. 1A).

Mitochondria were purified from day 5-transfected COS7 cells, lysed, and frataxin-associated molecules were immunoprecipitated by anti-frataxin antibody and analyzed by SDS/PAGE followed by silver staining. Three visible bands were cut from the gel and analyzed by mass spectrometry and the results are shown in Table 1. A few sporadic hits that occurred in non-mitochondrial proteins (A2M, COL1A2, KCTD3, CAD) were removed from the list. The remaining mitochondrial peptides were ranked first by the percent sequence coverage, and secondly by the number of hits (i.e. peptide fragments precipitated), because these both relate to the confidence in the interaction (Table 1). The chaperone GRP75/Mortalin/ HSPA9B, a mitochondrial stress-induced peptide, was at the top of the list, with 28% sequence coverage. The ISD11 homolog (CH6OFR149) was second on the list with 14% sequence coverage. ISD11 was recently identified to be a component of the Nfs1/ISCU complex of mitochondrial iron-sulfur cluster biogenesis (25,26). ATP5L, a component of the mitochondrial ATP

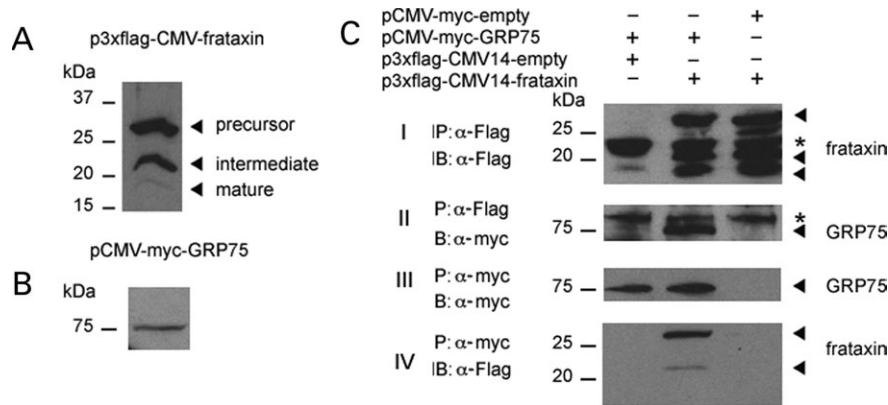


Figure 2. Frataxin interacts with GRP75. (A) p3 × flag-frataxin or (B) pCMV-myc-GRP75 plasmid was overexpressed in HEK293T cells. Lysate was analyzed by anti-flag antibody and three bands were recognized (A) or by anti-myc antibody (B). (C) Frataxin interacts with GRP75 *in vivo*. Interaction of GRP75 and frataxin was identified by co-immunoprecipitation. HEK293T cells were transiently transfected with the indicated plasmid. In tier I, Cell lysates were immunoprecipitated with an anti-flag antibody, followed by immunoblotting with anti-flag antibody. The presence of density in lanes 2 and 3 but not lane 1 demonstrates that the anti-flag antibody detects the three forms of flag epitope frataxin proteins. The asterisk indicates IgG light chain. In tier II, The increased density in lane 2 but not in lane 1 or 3 indicates that anti-flag antibody immunoprecipitates GRP75. The asterisk indicates a non-specific band. In tier III, cell lysates were immunoprecipitated with an anti-myc antibody, followed by immunoblotting with anti-myc antibody. The presence of density in lanes 1 and 2 but not lane 3 demonstrates that the anti-myc antibody detects the myc epitope and not anything else. In tier IV, the presence of bands in lane 2 but not lane 1 or 3 confirms a GRP75-frataxin interaction, similar to tier II, lane 2.

synthase, was third on the list with 11% coverage. Fourth on the list with 9% coverage was mitochondrial chaperone HSP60/SPG13, mutations of which cause hereditary spastic paraplegia (27). Also, HSP60 is known to interact with GRP75 and to participate in folding of translocated mitochondrial proteins (28). Fifth and sixth on the list at 7% coverage were ATAD3, a mitochondrial ATPase, and frataxin itself. Seventh on the list was succinate dehydrogenase, subunits of which have recently been shown to interact with frataxin (19,20), and eighth was AFG3L2, a mitochondrial protein partner of paraplegin (29,30). Thus, frataxin appears to interact with at least two other proteins, which either directly cause movement disorders or are their partners, i.e. HSP60/SPG13 and AFG3L2.

Frataxin interacts with GRP75/mortalin

The highest sequence coverage of immunoprecipitated proteins was for GRP75/mortalin, a mitochondrial chaperone and homolog of yeast chaperone ssq1, which participates in folding and insertion of iron-sulfur clusters in recently imported mitochondrial proteins (31). We confirmed an interaction between flag-tagged frataxin and myc-tagged GRP75 by a different set of co-immunoprecipitation epitopes (Fig. 2). In Figure 2A, three different bands were detected by anti-flag antibody in the HEK293T cells transfected with plasmid p3xflag-CMV-frataxin, three different bands indicated precursor frataxin, intermediate frataxin and mature form frataxin. And in Figure 2B, only one band was recognized by anti-myc antibody in the HEK293T cells transfected with pCMV-myc-GRP75. In Figure 2C, tier II, lane 2, it is demonstrated that a 75 kDa protein immunoprecipitated by anti-flag antibody is detected by anti-myc antibody. Conversely, Figure 2C tier IV demonstrates that a protein immunoprecipitated by anti-myc, which is only attached to GRP75, is detected by anti-flag antibody. Thus, it was demonstrated that frataxin interacts with GRP75 by immunoprecipitation and probing in both directions. In Figure 2C tiers I and III

are controls, demonstrating that the anti-flag (tier I) and anti-myc (tier III) antibodies are effective both for immunoprecipitation and immunoprecipitation.

ISD11 colocalizes with frataxin and is targeted to the mitochondria

ISD11 has recently been demonstrated in yeast to interact with both Nfs1 and ISCU of the mitochondrial iron-sulfur cluster biogenesis machinery (25), and so finding a mammalian ISD11 homolog as an interactor of frataxin was of particular interest.

If frataxin interacts with ISD11, the proteins should colocalize within cells. Frataxin and flag-tagged ISD11 constructs were co-transfected into COS7 cells. The expressed proteins were then stained with antibodies to frataxin and flag, respectively, and visualized by immunofluorescence microscopy. A merge of the two stains demonstrated colocalization (Fig. 3C), in a punctate, extranuclear distribution.

In addition to its known mitochondrial location, frataxin has recently been reported to occur outside the mitochondria (32,33). To experimentally determine the cellular compartment to which ISD11 localizes, we transfected p3 × flag-ISD11 into COS7 cells and stained mitochondria with MitoTracker red. The triple flag epitope was fused to the C terminus of ISD11 to allow normal processing of the putative mitochondrial leader sequence. The results clearly indicated that the ISD11-3 × flag fusion protein accumulates in the mitochondria (Fig. 3F). We produced the ISD11 poly-antibody in rabbit and this antibody could recognize both transfected ISD11 and endogenous ISD11, and western blot showed that endogenous ISD11 was localized on the mitochondria (Fig. 3G).

Frataxin interacts with ISD11 *in vitro*

To confirm the interaction between frataxin and ISD11, we performed pull-down experiments with recombinant

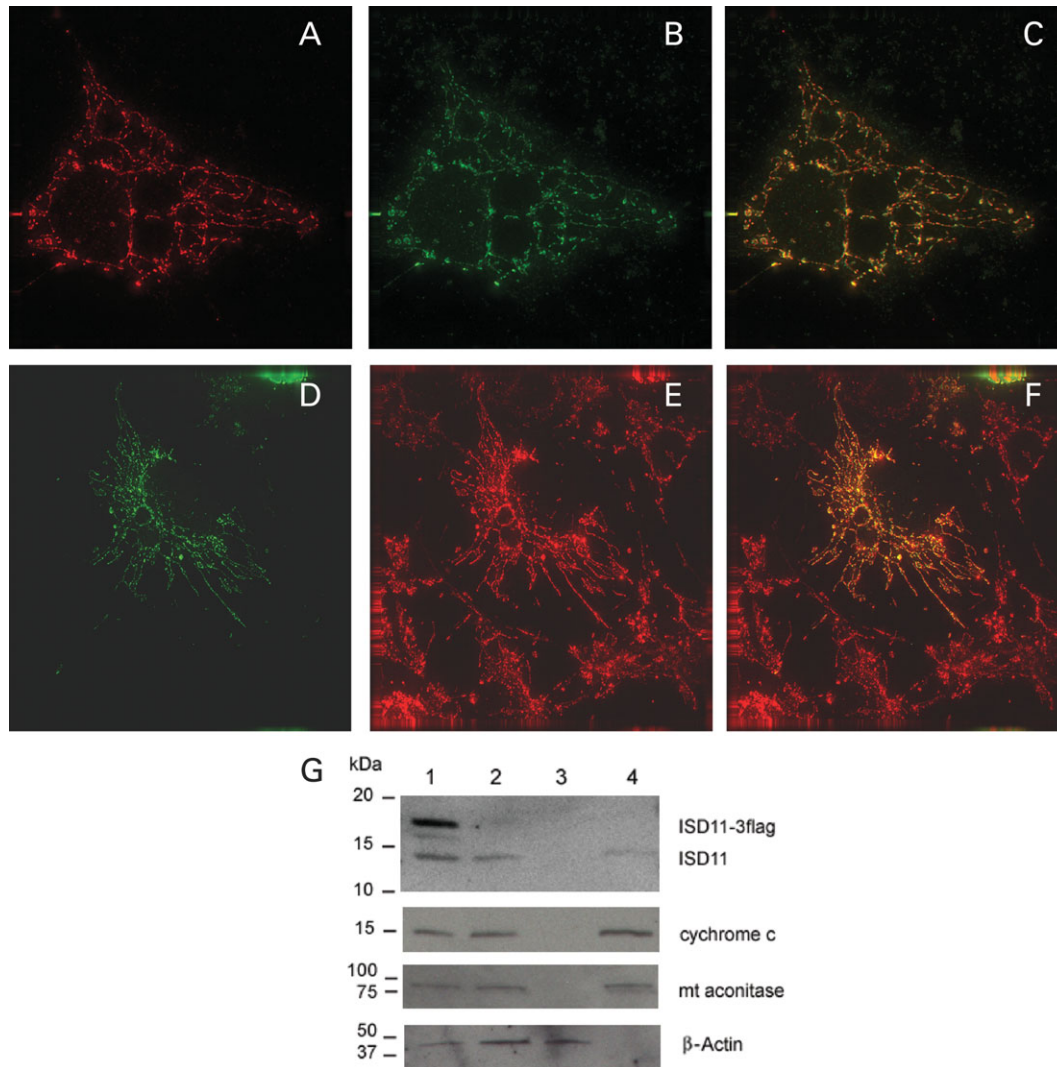


Figure 3. ISD11 colocalizes with frataxin and is targeted to the mitochondria in COS7 cells. COS7 cells were cultured on coverslips, transfected with p3 × flag-ISD11 and pcDNA3.1-frataxin-HA (A–C), and analyzed by immunofluorescence with monoclonal anti-flag/goat anti-mouse rhodamine (A) (red), rabbit anti-frataxin/goat anti-rabbit fluorescein conjugate (B) (green). (C) The merge of (A) and (B). In (D–E), COS7 were transfected with p3 × flag-ISD11 and analyzed by immunofluorescence with monoclonal anti-flag/goat anti-mouse FITC (D)(green) or Mitotracker(E)(red). (F) The merge of (D) and (E). (G) ISD11 is localized on mitochondria. Lane 1, whole cell lysate of 293T cells transfected with p3 × flag-ISD11, lane 2, whole cell lysate of 293T cells, lane 3 cytoplasm of 293T cells, lane 4, mitochondria lysate of 293T cells. The blot was probed with anti-ISD11, anti-cychrome C, anti-mitochondrial aconitase and β -actin antibody, respectively.

GST-tagged frataxin. As shown in Figure 4A, ISD11 bound to glutathione-Sepharose 4B beads containing GST- Δ 55frataxin (lane 3) but not to control glutathione-Sepharose 4B beads containing GST alone (lane 2).

Endogenous, unamplified frataxin protein interacts with ISD11 *in vivo*

We also confirmed an interaction between ISD11 and frataxin by a different set of co-immunoprecipitations (Fig. 4B–D). In Figure 4B (tier II, lane 2), it is demonstrated that a protein immunoprecipitated by anti-frataxin antibody is detected by anti-flag antibody, of which there is only one expressed, i.e. flag-ISD11. Conversely, Figure 4B tier IV demonstrates that a 15kDa protein immunoprecipitated by anti-flag in lane 1 is detected by anti-frataxin antibody. Since the cells were not transfected

with frataxin vector, we conclude that the 15 kDa protein identified by the anti-frataxin antibody is endogenous frataxin. A 17 kDa protein was immunoprecipitated by anti-flag in lane 2 and detected by anti-frataxin antibody exactly corresponds to the size we expect for frataxin plus the HA tag. Thus, it was demonstrated that frataxin interacts with ISD11 by immunoprecipitation and probing, in both directions. In Figure 4B tiers I and III are controls, demonstrating that the flag (tier I) and frataxin (tier III) antibodies are effective both for immunoprecipitation and immunoprobng.

We designed multiple experiments to test and therefore demonstrate that the interaction between frataxin and ISD11 was not the result of overexpression of frataxin.

After showing that ISD11 immunoprecipitates endogenous frataxin (Fig. 4B, Tier IV lane 1), we tested whether endogenous frataxin could immunoprecipitate ISD11; so we transfected

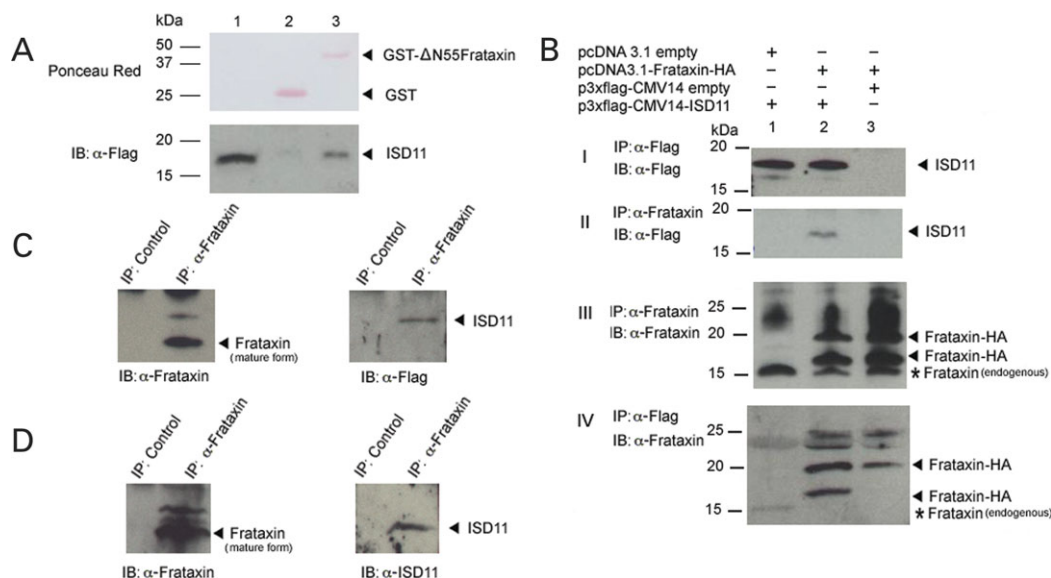


Figure 4. Frataxin interacts with ISD11. (A) Frataxin interacts with ISD11 *in vitro*. GST-Δ55frataxin pulls down ISD11-flag. HEK293T cells were transiently transfected with p3 × flag-ISD11. Expression of flag-tagged ISD11 is shown (lane 1). GST alone (lane 2) or GST-tagged frataxin (lane 3) were bound to beads and incubated with lysates of HEK293T cells transfected with p3 × flag-ISD11. Bead-bound protein complexes were subjected to immunoblotting and the blot was stained with Ponceau Red (upper tier) and probed with monoclonal anti-FLAG epitope antibody (bottom tier). (B) Frataxin interacts with ISD11 *in vivo*. Interaction of ISD11 frataxin was identified by co-immunoprecipitation. HEK293T cells were transiently transfected with the indicated plasmids. Tier I, cell lysates were immunoprecipitated with an anti-flag antibody, followed by immunoblotting with anti-flag antibody. The presence of density in lanes 1 and 2 but not lane 3 demonstrates that the anti-flag antibody detects the flag epitope and not anything else. In tier II, extracts from transfectants were immunoprecipitated with anti-frataxin and probed with anti-flag antibody. The increased density in lane 2 but not in 1 or lane 3 indicates that anti-frataxin antibody immunoprecipitates ISD11. In tier III, the extracts from the transfectants were immunoprecipitated with anti-frataxin and probed with anti-frataxin. In lane 1, the endogenous, mature, frataxin is visible, demonstrating that it is the major form immunoprecipitated and identified by the antibody. In tier III lanes 2 and 3, a strong signal of immediate form frataxin and mature form frataxin appended with the HA tag is also seen in addition to the endogenous, mature frataxin. In tier IV, extracts from the transfectants were immunoprecipitated with anti-flag antibody and immunoblotted with anti-frataxin antibody. In lane 1, in the absence of transfection, endogenous frataxin was immunoprecipitated by flag-tagged ISD11, demonstrating an interaction of ISD11 with endogenous, mature frataxin in the absence of frataxin overexpression. In tier IV lane 2, ISD11 interacts directly with mature frataxin, i.e. the 17 kD band is exactly the size expected for mature frataxin plus the HA tag, and is identified by the antibody as frataxin, confirming an ISD11-mature frataxin interaction. (C) Endogenous frataxin interacts with transfected ISD11. ISD11-flag only was immunoprecipitated by anti-frataxin antibody but not by normal rabbit serum. This occurred in the absence of transfected frataxin, demonstrating that endogenous frataxin is sufficient to produce a binding interaction with ISD11. (D) Endogenous frataxin interacts with endogenous ISD11. In an experiment with no transfections whatsoever, mitochondria were isolated from 30 confluent T75 flasks of HEK293T cells and lysed with Hepes buffer. The lysate was immunoprecipitated by normal rabbit serum or anti frataxin, and probed with anti-ISD11 antibody (5034) or anti-frataxin, respectively. Note that the endogenous frataxin pulls down ISD11 in the absence of overexpression of either frataxin or ISD11.

p3×flag-ISD11 vector into HEK293T cells, harvested and lysed cells. We immunoprecipitated the lysate with normal rabbit serum and anti-frataxin serum, respectively. Only anti-frataxin antibody precipitated ISD11-flag protein (Fig. 4C). No frataxin vector was transfected into HEK293T cells here, proving that ISD11-flag protein interacts with endogenous frataxin and is pulled down by anti-frataxin antibody.

Very recently, we produced an ISD11 polyclonal antibody in rabbit, and this antibody recognized both transfected ISD11 and endogenous ISD11 (Fig. 3G). To verify the interaction between endogenous frataxin and endogenous ISD11 in the absence of transfection of either gene, we isolated and lysed HEK293T mitochondria, immunoprecipitated with anti-frataxin antibody or normal rabbit serum, and then probed with ISD11 poly-antibody. Only anti-frataxin could immunoprecipitate ISD11 (Fig. 4D).

The interaction between frataxin and ISD11 is reversed by a chelator

As frataxin has been shown to bind metal ions, and specifically iron (34–37), we tested the influence of known chelators upon

the frataxin-ISD11 interaction. EDTA specifically decreased the interaction of ISD11 with frataxin, in a concentration-dependent fashion, i.e. the amount of ISD11 associated with the immunobeads is significantly lower in lysate with a buffer containing 1 and 10 mM EDTA (Fig. 5). Unexpectedly, the interaction of frataxin with ISD11 was inhibited by a buffer containing physiological concentrations (50 μM) of ferrous iron, and this interaction could be rescued by iron chelator desferrioxamine. The interaction was also inhibited by Ca²⁺, Mg²⁺, Mn²⁺, Cu²⁺, Co²⁺, Zn²⁺, Fe³⁺, but strikingly nickel, Ni²⁺, increased the interaction between frataxin and ISD11 (Fig. 5).

The frataxin point mutation I154F inhibits the interaction with ISD11, and is rescued by nickel

Most disease-causing alleles of frataxin are expansions of a GAA repeat in intron 1; however, multiple substitution mutations of frataxin also exist, which decrease protein function and cause FRDA. Using the pcDNA-frataxin-HA vector as a template, five of the known frataxin mutant constructs were generated: G130V, I154F, W155R, W173G and L156P. These constructs

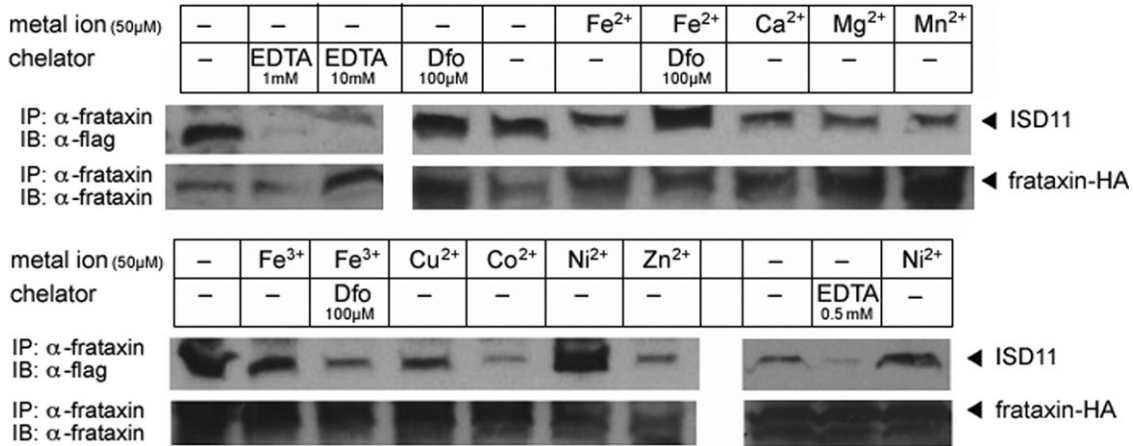


Figure 5. Binding of ISD11 to frataxin is increased by nickel but not iron. HEK293T cells were transfected with pcDNA3.1-frataxin-HA and p3 × flag-ISD11 and lysed/washed by HEPES buffer with correspond component above the figure. Cell lysates were immunoprecipitated with anti-frataxin antibody and immunoblotted with anti-flag antibody or anti-frataxin antibody. After immunoprecipitation, the beads were washed with the correspondent lysis buffer, respectively.

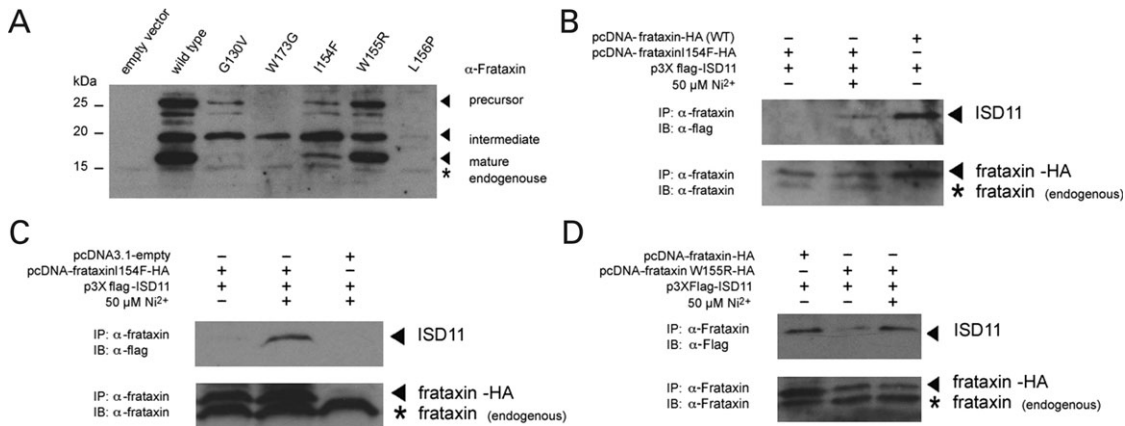


Figure 6. The interaction between ISD11 and frataxin mutants. (A) Expression of five point mutant frataxin in HEK293T cells. (B) The interaction between frataxin mutant I154F and ISD11. ISD11 and I154F were co-immunoprecipitated in HEPES buffer (lane 1) or HEPES buffer with 50 μM nickel (lane 2), the interaction between ISD11 and wild-type frataxin (lane 3). (C) Nickel rescues the interaction between frataxin I154F mutant and ISD11. ISD11 and I154F were co-immunoprecipitated in HEPES buffer (lane 1) or HEPES buffer with 50 μM nickel (lane 2). In lane 3, the pcDNA3.1 empty vector and ISD11 were co-immunoprecipitated in HEPES buffer with 50 μM nickel, producing no band, supporting the view that the interaction was dependent on the rescued interaction between frataxin I154F and ISD11. (D) The interaction between frataxin mutant W155R and ISD11. Only weak interaction was observed between W155R mutant and ISD11. Nickel could increase the interaction between ISD11 and W155R mutant.

were transfected into HEK293T cells, blotted and probed with anti-frataxin antibody. The mature form of frataxin was not expressed in the G130V, W173G and L156P mutations (Fig. 6A), suggesting that these mutations decrease mature protein expression. In contrast, the I154F and W155R construct produced a reasonable amount of the mature mitochondrial form of frataxin. The frataxin I154F mutant and ISD11 constructs were transfected into HEK293T cells, and their interaction was analyzed by co-immunoprecipitation. The results showed that no ISD11 was co-immunoprecipitated by frataxin antibody under these conditions (Fig. 6B, left lane). But when nickel was added into the HEPES buffer, a band was co-immunoprecipitated. (Fig. 6B, middle lane 2). To determine whether this band was immunoprecipitated by frataxin I154F contained on the plasmid, or the much lower level of endogenous wild-type cellular frataxin, we transfected pcDNA empty vector and ISD11

into HEK293 cells, and lysed the cells with HEPES buffer treated with and without nickel. If there were no interaction between I154F and ISD11, then we should observe the same bands in middle lane and right lane of Figure 6C. But we observed no band in right lane of Figure 6C, suggesting that nickel rescues the interaction between frataxin I154F and ISD11. For the W155R mutant, only weak interaction was observed between ISD11 and W155R mutant (Fig. 6D, middle lane). Nickel could partially rescue the interaction between ISD11 and W155R mutant (Fig. 6D, right lane).

Silencing ISD11 decreases aconitase and NFS1/ISCU and increases iron concentration

Frataxin knockdown in cells and animals produces both defects in iron–sulfur cluster enzyme activity, and cellular iron over-

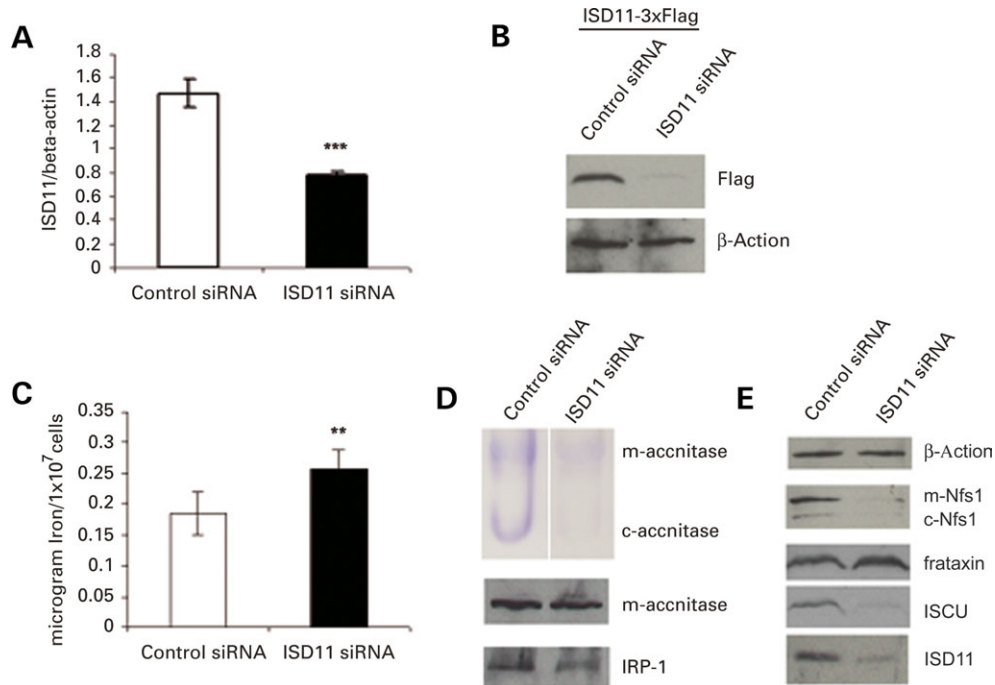


Figure 7. Silencing ISD11 decreases aconitase and Nfs1/ISCU and increases iron concentration. (A) HEK293T cells were transfected with ISD11 siRNA or control siRNA, mRNA prepared and analyzed by QPCR, using primers specific to the ISD11 gene, error bars represent standard deviation of four experiments. *** $P < 0.001$. (B) Western blot detection of ISD11-flag fusion protein, using anti-flag antibody, 48 h post-transfection with control siRNA or ISD11 siRNA. (C) Total cellular iron concentrations of HEK293T cells transfected with ISD11 siRNA or control siRNA. The experiment was repeated three times and ** $P < 0.005$. (D) Aconitase activity analysis of HEK cells transfected with Control siRNA or ISD11 siRNA. (E) Down-regulation of ISD11 affects Nfs1 and ISCU protein level.

load (10,23). If frataxin causes its effects on iron–sulfur cluster status through its interaction with ISD11, then the knockdown of ISD11 should produce the same consequences (i.e. phenocopy) as frataxin knockdown. siRNA directed against ISD11 or a scrambled control was transfected into the HEK293T cells. The anti-ISD11 siRNA resulted in a >50% reduction of the ISD11 mRNA relative to transfection with the control siRNA by quantitative RT–PCR (Fig. 7A). At the protein level, co-transfection of ISD11 siRNA and p3 × flag-ISD11 knocked down ISD11 protein expression in HEK293T cells (Fig. 7B). ISD11 siRNA also efficiently knocked down endogenous ISD11 protein in HEK293T cells (Fig. 7E).

We measured total cell iron content in siRNA transfected cells. Compared to the scrambled control siRNA transfected, the ISD11 siRNA transfected cells showed a significant increase in total iron content (Fig. 7C), as do Δyfh yeast cells (38). Aconitase activity also was examined in HEK293T cells depleted of ISD11. The results showed that ISD11 siRNA reduces both cytosolic and mitochondrial aconitase activities, even while the protein level of mitochondrial aconitase was similar, and IRP1 slightly decreased (Fig. 7D). Nfs1/ISCU protein expression was examined as well. The results showed that ISD11 siRNA reduces both cytosolic and mitochondrial Nfs1/ISCU level (Fig. 7E).

ISD11 mRNA levels decrease in FRDA patients

We have demonstrated that frataxin interacts with ISD11 and that ISD11 knockdown duplicated multiple consequences of

frataxin deficiency. Previously, we have demonstrated that ISCU and Nfs1 (ISCS) transcript levels are decreased in FRDA patients' cells (24). If frataxin and ISD11 interact at the protein level, we reasoned that their mRNAs might be co-regulated and we investigated this possibility by quantitative RT–PCR. The results showed ~75% reduction of the frataxin transcript and ~60% reduction of the ISD11 mRNA in FRDA patients (Fig. 8). Thus, frataxin-deficiency causes a transcriptional co-repression of multiple transcripts involved in iron–sulfur cluster biosynthesis, including ISD11, ISCU and Nfs1 (ISCS) in FRDA patients. This is expected if frataxin's primary function is in iron–sulfur cluster biosynthesis, and less expected if frataxin's primary function is in iron metabolism or transport.

DISCUSSION

Frataxin associates with multiple mitochondrial proteins

Deficiency of frataxin protein causes FRDA. Substantial debate about frataxin's primary physiological role still exists, and prime candidates include iron–sulfur cluster biogenesis and repair, iron transport and metabolism, and anti-oxidative action. We immunoprecipitated frataxin from mitochondrial extracts to isolate its partners, to help determine frataxin's most likely physiological role. Multiple mitochondrial proteins were isolated, which were consistent between lymphoblasts and COS7 cells, and some previous findings in

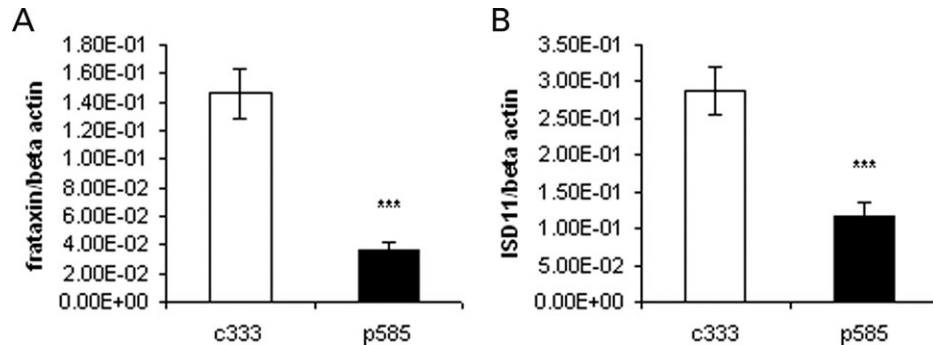


Figure 8. mRNA expression of frataxin and ISD11 in control (c333) and FRDA patient's (p585) lymphoblasts. The experiment was repeated three times. (A) Frataxin mRNA expression decreased in patient cells, *** $P < 0.001$. (B) ISD11 frataxin mRNA expression decreased in patient cells, too. *** $P < 0.001$.

yeast and worms, and are most consistent with a role of frataxin in iron–sulfur cluster biogenesis and chaperone function.

Frataxin interacts with the mitochondrial chaperone GRP75/mortalin

First, there were multiple hits in the mitochondrial chaperone protein GRP75/mortalin/HSPA9B (hereafter GRP75) suggesting that frataxin is well associated with a known mitochondrial chaperone. GRP75 is a known interactor of the mitochondrial chaperone HSP60/GroEL/SPG13/HSPD1 (28), the best represented interactor on the basis of peptides isolated (Table 1). Amino acids comparison analysis showed that there is 49% identity and 70% similarity between GRP75 and Ssq1. Ssq1 is a mitochondrial matrix protein which was shown to be essential for the import and maturation of the yeast frataxin homolog Yhf1 (39) and for iron–sulfur (Fe/S) clusters assembly in mitochondria (40); mutants in Ssq1 were reported to have low levels of Fe/S cluster-containing enzymes and accumulate iron within mitochondria (41). Also, Ssq1 interacts with Isu (the yeast ortholog of human ISCU) and Jac1 (31,42); and it is involved in iron–sulfur cluster biogenesis (31,43).

Frataxin associates with the mitochondrial chaperone HSP60

We observed several peptide interaction hits of frataxin with HSP60. HSP60 is a known interactor of GRP75, and together with HSP10 forms a mitochondrial chaperonin complex (44). HSP60 is a homolog of the well-known *E.Coli* GroEL (45). *In vitro* studies have shown that in *E.Coli* GroEL interacts with rhodanese (46), a mitochondrial enzyme involved in the repair of Fe/S clusters (47) transcript levels of which we have previously shown to be decreased in FRDA lymphoblasts (24). GroEL also inserts iron–sulfur cluster into adrenodoxin (48), a protein involved in electron transfer from NADPH+ (via a reductase) to cytochrome P-450 in the adrenal gland. And we also observe that adrenodoxin activity is deficient in frataxin-deficient cells (Napoli *et al.*, in preparation). In yeast, decreases of hsp60 cause iron increase and negatively affect the activity of Fe/S enzymes upon oxidative stress (49).

So, by inference from the combined yeast and mammalian studies, the interaction of frataxin with GRP75 and HSP60 is consistent with the idea that frataxin is part of a chaperone

complex that inserts iron–sulfur clusters into recently imported apoproteins (50). This association of frataxin with mitochondrial chaperones may help explain the interesting results of Bulteau *et al.* (15), who observed a stress-dependent association of frataxin with mitochondrial aconitase. If frataxin is already associated with mitochondrial chaperones, and upon stress these chaperones preferentially bind unfolded proteins, then the stress-dependent association of frataxin with aconitase may occur through linkage of each to mitochondrial chaperones.

Confirmation of the interaction of frataxin with succinate dehydrogenase

Our co-immunoprecipitation results from mitochondria of lymphoblasts and COS cells confirm the study of frataxin's partners in yeast and *C. elegans* (19,20), in which frataxin was observed to interact with succinate dehydrogenase. Succinate dehydrogenase is an enzyme complex embedded in the mitochondrial inner membrane, interacting with the matrix but not the intermembrane space. These results further localize frataxin's interactors to the mitochondrial matrix and matrix side of the mitochondrial inner membrane.

Frataxin interacts with an ISD11 ortholog

The second greatest sequence coverage of frataxin's interactors occurred with C6ORF149, an ortholog of yeast ISD11, which has recently been demonstrated to be a component of the eukaryotic Nfs1/ISCU iron–sulfur biogenesis complex (25,26). Frataxin physically interacts with ISD11 by several criteria, including immunoprecipitation in both directions, GST-pulldowns and colocalization within the mitochondria.

In yeast, frataxin interacts with Nfs1/ISCU, and this interaction is increased by ferrous iron (12). Unexpectedly, we observed that iron inhibited the interaction between ISD11 and frataxin, and that the iron-specific chelator desferoxamine could rescue the interaction. The chelator EDTA clearly inhibited the interaction between frataxin and ISD11 in a concentration-dependent manner, and so a survey of other metal ions was undertaken. We found that nickel at a 50 μ M concentration increased the interaction between frataxin and ISD11. Nickel is an essential nutrient for eukaryotes.

Some data have demonstrated that deficiency of nickel causes poor absorption of ferric iron (51), and in A549 cells, nickel treatment decreases total cellular iron level (52). Nickel forms Ni-Fe-S clusters in bacteria (53), and nickel 'bridges' 4-iron, 4-sulfur clusters on some peptides that act as scaffolds (54). So, the data suggest that nickel supports the interaction of frataxin and ISD11, and thus iron-sulfur cluster biogenesis.

The I154F and W155R mutations decrease the interaction between frataxin and ISD11

Approximately 4% of FRDA patients are compound heterozygotes. Three point mutations, G130V, I154F and W173G, were found in 40% of families with identified point mutations (55). We generated these three mutant frataxin plasmids and transfected them into HEK293T cells. Both G130V and W173G were poorly expressed in the mature form, suggesting that these two mutations affect expression, maturation, or degradation of frataxin. In contrast, the I154F mutant was well expressed as mature frataxin. However, the frataxin I154F mutation, even expressed at high levels, was not immunoprecipitable by ISD11, whereas normal frataxin was. Intriguingly, 50-micromolar nickel could rescue the interaction between the mutant frataxin and ISD11. This result suggests that the I154F mutation causes FRDA through defective interaction with ISD11. This suggests ISD11 is the functional binding partner of both frataxin and the Nfs1/ISCU complex.

Crystal structure analysis showed that frataxin protein is a compact $\alpha\beta$ sandwich (56) and none of FRDA point mutations overlap the proposed iron-binding region (17,57). The I154 residue is located on the central β sheet, β_4 , which we propose contains the interaction surface with ISD11. We generated other point mutations occurring on the β_4 sheet and causing FRDA, W155R and L156P (55,58); we found that only the W155R mutant was well expressed as mature frataxin, and the W155R mutant only weakly interacts with ISD11. Fifty-micromolar nickel could increase the interaction between the mutant frataxin and ISD11. Nickel could cause increased interaction between frataxin and ISD11 either through bridging their interaction or by stabilizing mutant frataxin.

siRNA against ISD11 phenocopies multiple aspects of frataxin deficiency

If frataxin's upstream interaction with ISD11 is necessary for NFS1/ISCU function, then conversely silencing ISD11 should phenocopy the same consequences of frataxin depletion, which include iron-sulfur cluster deficiency and iron accumulation. We silenced the ISD11 by siRNA in HEK293T cells. Our results showed that when ISD11 was depleted by siRNA, both mitochondrial and cytosolic aconitase activity decreased, and that this was not a consequence of decreased protein levels. ISD11 silencing also decreased both the mitochondrial and cytosolic forms of the Nfs1/ISCU protein, suggesting that ISD11 functions in both compartments. Although either deficiency of frataxin or ISD11 affects the Nfs1/ISCU complex, knockdown of ISD11 did not cause a deficiency of frataxin mRNA or protein. We suggest that

frataxin deficiency causes mitochondrial and cytosolic aconitase deficiency through the defective interaction with ISD11.

A function for frataxin in iron-sulfur cluster biogenesis

In *Escherichia coli*, the CyaY protein (the bacterial ortholog of frataxin) is thought to specifically interact with IscS (Nfs1) to donate iron to build [2Fe-2S] on the scaffold IscU (59). But up to now no interaction has been observed between frataxin and Nfs1 in human cells (14). Isd11 exists only in eukaryotes (60). Our data demonstrate that frataxin interacts with ISD11, which is essential for the proper function of the Nfs1/ISCU complex (25,26). The data presented here support the view that ISD11 serves as an adaptor between frataxin and Nfs1/ISCU. This is consistent with our previous work in cells from FRDA patients showing that the mRNA and protein level of Nfs1 and ISCU were decreased in frataxin-deficient cells (24).

There has been substantial debate over the role of frataxin, including iron transport, iron bioavailability, antioxidant status, mitochondrial stimulator and iron-sulfur cluster function. Data presented here suggest that in human cells, frataxin is directly associated with ISD11 of the iron-sulfur cluster biogenesis complex, and that two mutations that cause FRDA decrease this specific interaction, and that nickel increases it. Furthermore, there is interaction of frataxin with both GRP75 (an ssq1 homolog) and HSP60, and it has previously been shown in yeast that the chaperone system is essential for insertion of iron-sulfur clusters into newly imported mitochondrial proteins. These data strongly support a direct role of frataxin function in iron-sulfur cluster biogenesis and insertion into apoproteins as part of a mitochondrial chaperone complex (Fig. 9).

MATERIALS AND METHODS

Biochemical reagents were purchased from Sigma (St Louis, MO, USA), Bio-Rad (Hercules, CA, USA) or mentioned in the text.

Cell culture

All cells were maintained at 37°C in a humidified atmosphere containing 5% CO₂. Lymphocytes were grown as described (61). COS7 and HEK293T cells (from ATCC) were grown in DMEM medium (Gibco-BRL) supplemented with 10% fetal bovine serum, 1 mM sodium pyruvate and penicillin/streptomycin.

Plasmid constructs and site-directed mutagenesis

Open reading frame sequence with C-terminal flag sequence (gactacaaggacgacgatgacaagtaa) of Human frataxin cDNA (GenBank Accession No. NM_000144) was created by PCR and inserted into pcDNA3.1; mature frataxin sequence (nucleotide 521-988) was inserted into pGEX-4T-1 (Amersham Pharmacia Biotech) to produce GST- Δ N55-frataxin fusion protein. Frataxin cDNAs also was inserted in-frame into p3 \times flag-CMV-14 (Sigma). The pcDNA-frataxin-HA construct

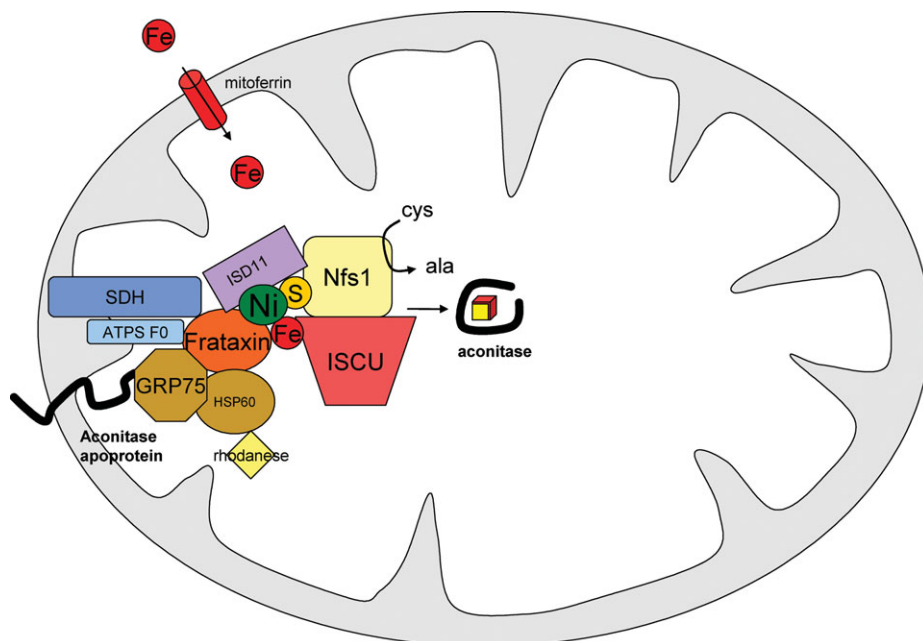


Figure 9. A cartoon for the proposed function of the frataxin in iron-sulfur cluster insertion into apoproteins. Frataxin's interactors include the chaperones GRP75 and HSP60, and the inner mitochondrial membrane proteins succinate dehydrogenase and ATP synthase F0. Frataxin also interacts with ISCU, in an iron-dependent fashion. Frataxin interacts with ISD11 of the Nfs1 complex in a nickel-dependent fashion. Sulfur is derived from cysteine by Nfs1. Nickel is known to bind sulfur atoms and bridge iron-sulfur clusters on peptides (see Discussion). Since frataxin interacts both with components of the chaperone system and with the components of iron-sulfur cluster biogenesis, it is proposed that frataxin supports the functions of iron-sulfur cluster insertion into apoproteins.

was described previously (62). G130V, I154F, W155R, L156P and W173G mutants of frataxin were obtained from pcDNA-frataxin-HA by site-directed mutagenesis using the QuikChange site-directed mutagenesis kit (Stratagene) and all mutants were sequenced to confirm their sequences. GRP75 cDNAs (GenBank Accession No. NM_004134) was inserted in-frame into pCMV-myc(Clontech), ISD11 cDNAs (GenBank Accession No. NM_020408) was inserted in-frame into p3 × flag-CMV-14.

Frataxin pull-down and mass spectrometry

Pull-down and mass spectrometry experiments were carried out in control lymphoblasts (about 1×10^9 cells) and COS7 cells. Eighteen T75 flasks of COS7 (90% confluence) were transfected with 430 μ g of pcDNA-frataxin-flag plasmid constructs using Lipofectamine 2000 (Invitrogen) in the serum-free medium. After 4 h of incubation, medium was replaced with fresh complete medium, and cells were cultured for an additional 96 h before collection.

Mitochondria from COS7 and lymphoblasts were isolated as before (24), treated with a lysis buffer (50 mM Tris, pH 8.0, 150 mM NaCl, 1 mM PMSF, 1% IGEPAL CA-630 (Sigma), at 4°C for 30 min and insoluble material removed by centrifugation. Protein concentration was estimated using the Bradford assay (Bio-Rad). Frataxin protein complexes were immunoprecipitated by rabbit polyclonal anti-frataxin antibody and rProtein G Agarose (Invitrogen). The immunoprecipitated samples were analyzed by Coomassie blue (lymphoblasts) and silver stain kit (Invitrogen) (COS7) and mass spectrometry analysis (Molecular Structure Facility, McDavis, CA).

Preparation of recombinant proteins

The recombinant glutathione-S-transferase (GST) tagged proteins were expressed in *E. coli* strain BL21-Star (DE3)(Invitrogen) with 0.5 mM isopropyl- β -L-thiogalactopyranoside (IPTG) at 22°C overnight. Cells were collected and lysed in PBS buffer (pH 7.4), supplemented with 1% TritonX-100, 10 mM DTT, 0.5 mM PMSF and 1 mg/ml lysozyme. After incubation on ice for 30 min, the samples were centrifuged and the supernatants were purified using glutathione-S-Spharose beads (Amersham Biosciences).

Antibody production

The rabbit polyclonal antibody 5034 was raised against synthetic multiple antigenic peptide corresponding 55–72 amino acid residues (LVNKAKRDLGVIRRQVHI) of human ISD11. Antiserum was generated in New Zealand white rabbits by Bio-synthesis Inc. (Lewisville, TX).

Western blot analysis

Forty microgram whole cell lysate, or 40 μ g cytoplasmic protein or 15–20 μ g mitochondrial protein was analyzed on 15% SDS-PAGE. Electrophoresis was carried out at 130 V for about 1 h following a low voltage of 80 V for 10 min. After electrophoresis, the proteins were transferred to nitrocellulose membranes using a Mini Trans-Blot cell (Bio-rad). The membranes were blocked with 4% non-fat milk in Tris-buffered saline with 0.1% Tween 20 for 1 h. subsequently, the membranes were incubated overnight with the following

primary antibodies: rabbit anti-frataxin; rabbit anti-ISCU and rabbit anti-Nfs1 (kind gifts from Drs Tracey Rouault and Wing Hang Tong); rabbit anti-IRP1 (Santa Cruz Biotechnology) and rabbit anti-mitochondrial aconitase (a kind gift from Dr Luke Szweda); rabbit anti-ISD11; mouse anti- β -actin; mouse anti-cytochrome c (MitoScience), mouse anti-flag (Sigma), mouse anti-myc (Roche). Afterwards, the membranes were developed with AP-conjugated secondary antibodies using a chemiluminescent substrate (Bio-rad).

Glutathione-S-transferase pull-down assay

A total of 2.5×10^6 HEK293T cells were seeded in 60 mm dishes. After overnight growth, cells were 80% confluent and transfected with 8 μ g p3 \times flag-ISD11 plasmid using Lipofectamine 2000 (Invitrogen) in serum-free medium. After 4 h of incubation, medium was replaced with fresh complete medium, and cells were cultured for an additional 48 h before collection. The cells were lysed in TBS buffer [50 mM TrisHCl, 150 mM NaCl, 1% TritonX-100, 1 mM PMSF and EDTA-free complete protease inhibitor cocktail (Roche)]. Binding assays were precleared by incubating cell extracts in TBS buffer with 25 μ g GST and 40 μ l glutathione-S-Sepharose beads for 1 h at 4°C, and the supernatant was incubated with 10 μ g GST- Δ N55frataxin or GST protein bound to 40 μ l glutathione-S-Sepharose beads for 3 h at 4°C. After three washes with TBS buffer, the bound proteins were analyzed by western blot.

Co-immunoprecipitation assays

HEK293T cells was transfected with correspond plasmids and culture for 72 h. The cells were lysed with Hepes buffer (pH7.5, containing 20 mM Hepes, 150 mM KCl, 0.5% TritonX-100, 10% (v/v) glycerol, 1 mM phenylmethylsulfonyl fluoride and EDTA-free complete protease inhibitor cocktail (Roche) with/without 50 μ M ferrous chloride or other metal ion. The whole cell lysates were incubated with ANTI-FLAG-M2 resin (Sigma), Anti-c-Myc Agarose (Sigma) or rabbit polyclonal anti-frataxin antibody and rProtein G Agarose at 4°C, rotated overnight and washed four times with lysis buffer. Precipitates were analyzed by Western blotting using anti-flag mAb, anti-myc mAb or rabbit polyclonal anti-frataxin antibody. Antibodies were detected as above.

Immunofluorescence analysis

COS7 cells were plated on coverslips in six well plates. For mitochondria localization, p3 \times flag-ISD11 was transfected into COS7 cells cultured for 24 h, exposed to 100 nM MitoTracker Red CMX (Molecular probe) for 1 h at 37°C and then fixed in 3.7% paraformaldehyde for 30 min at 4°C and prechilled methanol 10 min at -20°C. After washing once with PBS, the cells were permeabilized with 0.25% Triton X-100/PBS for 5 min, and then washed three times in PBS followed by blocking in fresh 1% BSA/PBS for 30 min at 37°C. Then the cells were incubated with the primary antibody at 4°C overnight. The primary antibody consisted of anti-flag mAb. After overnight incubation, the coverslips were rinsed

three \times in PBS and reacted for 1 h with goat anti-mouse fluorescein (Jackson ImmunResearch) in the dark. Cells were washed three times in PBS mix in mounting media. For colocalization of frataxin and ISD11, pcDNA-frataxin-HA and p3 \times flag-ISD11 were co-transfected into COS7 cells. The primary antibodies were consisted of the rabbit polyclonal anti-frataxin antibody and anti-flag mAb. Secondary antibodies were goat anti-rabbit fluorescein conjugate (Jackson ImmunResearch) and goat anti-mouse rhodamine (Jackson ImmunResearch). All samples were imaged using DeltaVision microscope (APLLC).

Quantitative RT-PCR analysis

Total RNA was prepared using Qiagen Mini Kit (Qiagen, CA, USA), and RNA concentration was determined by UV spectrophotometry. Reverse transcription of 5 μ g RNA was performed using an RT-PCR kit (Invitrogen, Gaithersburg, MD, USA), and reactions were performed in a 20 μ l volume. Two microlitres cDNA from 20 \times dilution of RT reaction were used for PCR. Quantitative PCR standard curves were set up for ISD11, frataxin and beta-actin, which method was previously described (63). The primers of PCR are as follows: β -actin forward, 5'-GCC AAC ACA GTG CTG TCT GG-3'; reverse, 5'-CTG CTT GCT GAT CCA CAT CTG C-3'; frataxin forward, 5'-AAA TCT GGA ACT TTG GGC CAC, reverse, 5'-ACC TCA GCT GCA TAA TGA AGC-3'; ISD11 forward, 5'-GAG AGA GCA AGC GTT TCA GC-3'; reverse, 5'-CTA GGT CCT GGG CAT GTC TC-3'. The PCR reaction and normalization were previously described in detail (62).

RNA interference (RNAi), total cellular iron measurement and aconitase activities

ISD11 short interfering RNAi oligonucleotides and Negative control oligonucleotides pools were purchased from Dharmacon (Denver, CO). HEK293T cells at a confluency of 30–50% were transfected with 100 nM siRNA using Lipofectamine 2000 (Invitrogen) every 72 h for 3–9 days (64), total cellular iron was determined under reducing conditions with Ferrozine as chelator, reactions were carried on in disposable 2.0 ml polypropylene tubes with screw caps from Sarstedt (65). Aconitase activity was analyzed in aconitase activity gels (66).

Statistics

Statistical analysis of the data was performed by Student's *t*-test.

ACKNOWLEDGEMENTS

This work was supported by grants from the USPHS/NIH: AG16719, AG11967 and EY12245 to G.A.C.; we thank C Song, WH Tong, YJ Dang and R Schoenfeld for the helpful suggestions.

Conflict of Interest statement. None declared.

REFERENCES

- Harding, A.E. (1981) Early onset cerebellar ataxia with retained tendon reflexes: a clinical and genetic study of a disorder distinct from Friedreich's ataxia. *J. Neurol. Neurosurg. Psychiatry*, **44**, 503–508.
- Harding, A.E. and Hewer, R.L. (1983) The heart disease of Friedreich's ataxia: a clinical and electrocardiographic study of 115 patients, with an analysis of serial electrocardiographic changes in 30 cases. *Q. J. Med.*, **52**, 489–502.
- Finocchiaro, G., Baio, G., Micossi, P., Pozza, G. and di Donato, S. (1988) Glucose metabolism alterations in Friedreich's ataxia. *Neurology*, **38**, 1292–1296.
- Campuzano, V., Montermini, L., Molto, M.D., Pianese, L., Cossee, M., Cavalcanti, F., Monros, E., Rodius, F., Duclos, F., Monticelli, A. *et al.* (1996) Friedreich's ataxia: autosomal recessive disease caused by an intronic GAA triplet repeat expansion. *Science*, **271**, 1423–1427.
- Sakamoto, N., Chastain, P.D., Parniewski, P. and Ohshima, K. (1999) Sticky DNA: self-association properties of long GAA.TTC repeats in R.R.Y triplex structures from Friedreich's ataxia. *Mol. Cell*, **3**, 465–475.
- Burnett, R., Melander, C., Puckett, J.W., Son, L.S., Wells, R.D., Dervan, P.B. and Gottesfeld, J.M. (2006) DNA sequence-specific polyamides alleviate transcription inhibition associated with long GAA.TTC repeats in Friedreich's ataxia. *Proc. Natl. Acad. Sci. USA*, **103**, 11497–11502.
- Herman, D., Jenssen, K., Burnett, R., Soragni, E., Perlman, S.L. and Gottesfeld, J.M. (2006) Histone deacetylase inhibitors reverse gene silencing in Friedreich's ataxia. *Nat. Chem. Biol.*, **2**, 551–558.
- Bidichandani, S.I., Ashizawa, T. and Patel, P.I. (1998) The GAA triplet-repeat expansion in Friedreich ataxia interferes with transcription and may be associated with an unusual DNA structure. *Am. J. Hum. Genet.*, **62**, 111–121.
- Montermini, L., Kish, S.J., Jiralerspong, S., Lamarche, J.B. and Pandolfo, M. (1997) Somatic mosaicism for Friedreich's ataxia GAA triplet repeat expansions in the central nervous system. *Neurology*, **49**, 606–610.
- Foury, F. (1999) Low iron concentration and aconitase deficiency in a yeast frataxin homologue deficient strain. *FEBS Lett.*, **456**, 281–284.
- Yoon, T. and Cowan, J.A. (2003) iron-sulfur cluster biosynthesis. Characterization of frataxin as an iron donor for assembly of [2Fe-2S] clusters in ISU-type proteins. *J. Am. Chem. Soc.*, **125**, 6078–6094.
- Gerber, J., Muhlenhoff, U. and Lill, R. (2003) An interaction between frataxin and Isu1/Nfs1 that is crucial for Fe/S cluster synthesis on Isu1. *EMBO Rep.*, **4**, 906–911.
- O'Neill, H.A., Gakh, O. and Isaya, G. (2005) Supramolecular assemblies of human frataxin are formed via subunit-subunit interactions mediated by a non-conserved amino-terminal region. *J. Mol. Biol.*, **345**, 433–439.
- Napoli, E., Taroni, F. and Cortopassi, G.A. (2006) Frataxin, iron-sulfur clusters, heme, ROS, and aging. *Antioxid. Redox. Signal.*, **8**, 506–516.
- Bulteau, A.L., O'Neill, H.A., Kennedy, M.C., Ikeda-Saito, M., Isaya, G. and Szewda, L.I. (2004) Frataxin acts as an iron chaperone protein to modulate mitochondrial aconitase activity. *Science*, **305**, 242–245.
- Lesuisse, E., Santos, R., Matzanke, B.F., Knight, S.A., Camadro, J.M. and Dancis, A. (2003) Iron use for haeme synthesis is under control of the yeast frataxin homologue (Yfh1). *Hum. Mol. Genet.*, **12**, 879–889.
- He, Y., Alam, S.L., Proteasa, S.V., Zhang, Y., Lesuisse, E., Dancis, A. and Stemmler, T.L. (2004) Yeast frataxin solution structure, iron binding, and ferredoxin interaction. *Biochemistry*, **43**, 16254–16262.
- Yoon, T. and Cowan, J.A. (2004) Frataxin-mediated iron delivery to ferredoxin in the final step of heme biosynthesis. *J. Biol. Chem.*, **279**, 25943–25946.
- Gonzalez-Cabo, P., Vazquez-Manrique, R.P., Garcia-Gimeno, M.A., Sanz, P. and Palau, F. (2005) Frataxin interacts functionally with mitochondrial electron transport chain proteins. *Hum. Mol. Genet.*, **14**, 2091–2098.
- Vazquez-Manrique, R.P., Gonzalez-Cabo, P., Ros, S., Aziz, H., Baylis, H.A. and Palau, F. (2006) Reduction of *Caenorhabditis elegans* frataxin increases sensitivity to oxidative stress, reduces lifespan, and causes lethality in a mitochondrial complex II mutant. *FASEB J.*, **20**, 172–174.
- Muhlenhoff, U., Richhardt, N., Ristow, M., Kispal, G. and Lill, R. (2002) The yeast frataxin homolog Yfh1p plays a specific role in the maturation of cellular Fe/S proteins. *Hum. Mol. Genet.*, **11**, 2025–2036.
- Anderson, P.R., Kirby, K., Hilliker, A.J. and Phillips, J.P. (2005) RNAi-mediated suppression of the mitochondrial iron chaperone, frataxin, in *Drosophila*. *Hum. Mol. Genet.*, **14**, 3397–3405.
- Puccio, H., Simon, D., Cossee, M., Criqui-Filipe, P., Tiziano, F., Melki, J., Hindelang, C., Matyas, R., Rustin, P. and Koenig, M. (2001) Mouse models for Friedreich ataxia exhibit cardiomyopathy, sensory nerve defect and Fe-S enzyme deficiency followed by intramitochondrial iron deposits. *Nat. Genet.*, **27**, 181–186.
- Tan, G., Napoli, E., Taroni, F. and Cortopassi, G. (2003) Decreased expression of genes involved in sulfur amino acid metabolism in frataxin-deficient cells. *Hum. Mol. Genet.*, **12**, 1699–1711.
- Adam, A.C., Bornhovd, C., Prokisch, H., Neupert, W. and Hell, K. (2006) The Nfs1 interacting protein Isd11 has an essential role in Fe/S cluster biogenesis in mitochondria. *EMBO J.*, **25**, 174–183.
- Wiedemann, N., Urzica, E., Guiard, B., Muller, H., Lohaus, C., Meyer, H.E., Ryan, M.T., Meisinger, C., Muhlenhoff, U., Lill, R. *et al.* (2006) Essential role of Isd11 in mitochondrial iron-sulfur cluster synthesis on Isu scaffold proteins. *EMBO J.*, **25**, 184–195.
- Hansen, J.J., Durr, A., Cournu-Rebeix, I., Georgopoulos, C., Ang, D., Nielsen, M.N., Davoine, C.S., Brice, A., Fontaine, B., Gregersen, N. *et al.* (2002) Hereditary spastic paraplegia SPG13 is associated with a mutation in the gene encoding the mitochondrial chaperonin Hsp60. *Am. J. Hum. Genet.*, **70**, 1328–1332.
- Wadhwa, R., Takano, S., Kaur, K., Aida, S., Yaguchi, T., Kaul, Z., Hirano, T., Taira, K. and Kaul, S.C. (2005) Identification and characterization of molecular interactions between mortalin/mtHsp70 and HSP60. *Biochem. J.*, **391**, 185–190.
- Banfi, S., Bassi, M.T., Andolfi, G., Marchitello, A., Zanotta, S., Ballabio, A., Casari, G. and Franco, B. (1999) Identification and characterization of AFG3L2, a novel paraplegin-related gene. *Genomics*, **59**, 51–58.
- Atorino, L., Silvestri, L., Koppen, M., Cassina, L., Ballabio, A., Marconi, R., Langer, T. and Casari, G. (2003) Loss of m-AAA protease in mitochondria causes complex I deficiency and increased sensitivity to oxidative stress in hereditary spastic paraplegia. *J. Cell. Biol.*, **163**, 777–787.
- Dutkiewicz, R., Schilke, B., Kniesner, H., Walter, W., Craig, E.A. and Marszalek, J. (2003) Ssq1, a mitochondrial Hsp70 involved in iron-sulfur (Fe/S) center biogenesis. Similarities to and differences from its bacterial counterpart. *J. Biol. Chem.*, **278**, 29719–29727.
- Acquaviva, F., De Biase, I., Nezi, L., Ruggiero, G., Tatangelo, F., Pisano, C., Monticelli, A., Garbi, C., Acquaviva, A.M. and Coccozza, S. (2005) Extra-mitochondrial localisation of frataxin and its association with IscU1 during enterocyte-like differentiation of the human colon adenocarcinoma cell line Caco-2. *J. Cell. Sci.*, **118**, 3917–3924.
- Condo, I., Ventura, N., Malisan, F., Tomassini, B. and Testi, R. (2006) A pool of extramitochondrial frataxin that promotes cell survival. *J. Biol. Chem.*, **281**, 16750–16756.
- Adamec, J., Rusnak, F., Owen, W.G., Naylor, S., Benson, L.M., Gacy, A.M. and Isaya, G. (2000) Iron-dependent self-assembly of recombinant yeast frataxin: implications for Friedreich ataxia. *Am. J. Hum. Genet.*, **67**, 549–562.
- Gakh, O., Adamec, J., Gacy, A.M., Twesten, R.D., Owen, W.G. and Isaya, G. (2002) Physical evidence that yeast frataxin is an iron storage protein. *Biochemistry*, **41**, 6798–6804.
- Park, S., Gakh, O., O'Neill, H.A., Mangravita, A., Nichol, H., Ferreira, G.C. and Isaya, G. (2003) Yeast frataxin sequentially chaperones and stores iron by coupling protein assembly with iron oxidation. *J. Biol. Chem.*, **278**, 31340–31351.
- Nichol, H., Gakh, O., O'Neill, H.A., Pickering, I.J., Isaya, G. and George, G.N. (2003) Structure of frataxin iron cores: an X-ray absorption spectroscopic study. *Biochemistry*, **42**, 5971–5976.
- Tamarit, J., Irazusta, V., Moreno-Cermeno, A. and Ros, J. (2006) Colorimetric assay for the quantitation of iron in yeast. *Anal. Biochem.*, **351**, 149–151.
- Voisine, C., Schilke, B., Ohlson, M., Beinert, H., Marszalek, J. and Craig, E.A. (2000) Role of the mitochondrial Hsp70s, Ssc1 and Ssq1, in the maturation of Yfh1. *Mol. Cell. Biol.*, **20**, 3677–3684.
- Lutz, T., Westermann, B., Neupert, W. and Herrmann, J.M. (2001) The mitochondrial proteins Ssq1 and Jac1 are required for the assembly of iron sulfur clusters in mitochondria. *J. Mol. Biol.*, **307**, 815–825.
- Knight, S.A., Sepuri, N.B., Pain, D. and Dancis, A. (1998) Mt-Hsp70 homolog, Ssc2p, required for maturation of yeast frataxin and mitochondrial iron homeostasis. *J. Biol. Chem.*, **273**, 18389–18393.
- Dutkiewicz, R., Schilke, B., Cheng, S., Kniesner, H., Craig, E.A. and Marszalek, J. (2004) Sequence-specific interaction between mitochondrial Fe-S scaffold protein Isu and Hsp70 Ssq1 is essential for their *in vivo* function. *J. Biol. Chem.*, **279**, 29167–29174.

43. Dutkiewicz, R., Marszalek, J., Schilke, B., Craig, E.A., Lill, R. and Muhlenhoff, U. (2006) The Hsp70 chaperone Ssq1p is dispensable for iron–sulfur cluster formation on the scaffold protein Isu1p. *J. Biol. Chem.*, **281**, 7801–7808.
44. Lin, K.M., Lin, B., Lian, I.Y., Mestrlil, R., Scheffler, I.E. and Dillmann, W.H. (2001) Combined and individual mitochondrial HSP60 and HSP10 expression in cardiac myocytes protects mitochondrial function and prevents apoptotic cell deaths induced by simulated ischemia-reoxygenation. *Circulation*, **103**, 1787–1792.
45. Fink, A.L. (1999) Chaperone-mediated protein folding. *Physiol. Rev.*, **79**, 425–449.
46. Ybarra, J., Bhattacharyya, A.M., Panda, M. and Horowitz, P.M. (2003) Active rhodanese lacking nonessential sulfhydryl groups contains an unstable C-terminal domain and can be bound, inactivated, and reactivated by GroEL. *J. Biol. Chem.*, **278**, 1693–1699.
47. Bonomi, F., Pagani, S., and Kurtz, D.M., Jr. (1985) Enzymic synthesis of the 4Fe-4S clusters of *Clostridium pasteurianum* ferredoxin. *Eur. J. Biochem.*, **148**, 67–73.
48. Iametti, S., Bera, A.K., Vecchio, G., Grinberg, A., Bernhardt, R. and Bonomi, F. (2001) GroEL-assisted refolding of adrenodoxin during chemical cluster insertion. *Eur. J. Biochem.*, **268**, 2421–2429.
49. Cabisco, E., Belli, G., Tamarit, J., Echave, P., Herrero, E. and Ros, J. (2002) Mitochondrial Hsp60, resistance to oxidative stress, and the labile iron pool are closely connected in *Saccharomyces cerevisiae*. *J. Biol. Chem.*, **277**, 44531–44538.
50. Schilke, B., Williams, B., Knieszner, H., Puksza, S., D’Silva, P., Craig, E.A. and Marszalek, J. (2006) Evolution of mitochondrial chaperones utilized in Fe-S cluster biogenesis. *Curr. Biol.*, **16**, 1660–1665.
51. Anke, M., Groppel, B., Kronemann, H. and Grün, M. (1984) Nickel—an essential element. In Sunderman, F.W., Jr. (Ed.), *Nickel in the Human Environment*. IARC Sci. Publ. 53, Lyon, pp. 339–365.
52. Chen, H., Davidson, T., Singleton, S., Garrick, M.D. and Costa, M. (2005) Nickel decreases cellular iron level and converts cytosolic aconitase to iron-regulatory protein 1 in A549 cells. *Toxicol. Appl. Pharmacol.*, **206**, 275–287.
53. Mulrooney, S.B. and Hausinger, R.P. (2003) Nickel uptake and utilization by microorganisms. *FEMS Microbiol. Rev.*, **27**, 239–261.
54. Laplaza, C.E. and Holm, R.H. (2002) Stability and nickel binding properties of peptides designed as scaffolds for the stabilization of Ni(II)-Fe(4)S(4) bridged assemblies. *J. Biol. Inorg. Chem.*, **7**, 451–460.
55. Cossee, M., Durr, A., Schmitt, M., Dahl, N., Trouillas, P., Allinson, P., Kostrzewa, M., Nivelon-Chevallier, A., Gustavson, K.H., Kohlschütter, A. *et al.* (1999) Friedreich’s ataxia: point mutations and clinical presentation of compound heterozygotes. *Ann. Neurol.*, **45**, 200–206.
56. Dhe-Paganon, S., Shigeta, R., Chi, Y.I., Ristow, M. and Shoelson, S.E. (2000) Crystal structure of human frataxin. *J. Biol. Chem.*, **275**, 30753–30756.
57. Nair, M., Adinolfi, S., Pastore, C., Kelly, G., Temussi, P. and Pastore, A. (2004) Solution structure of the bacterial frataxin ortholog, CyaY: mapping the iron binding sites. *Structure*, **12**, 2037–2048.
58. Labuda, M., Poirier, J. and Pandolfo, M. (1999) A missense mutation (W155R) in an American patient with Friedreich Ataxia. *Hum. Mutat.*, **13**, 506–506.
59. Layer, G., Ollagnier-de Choudens, S., Sanakis, Y. and Fontecave, M. (2006) iron–sulfur cluster biosynthesis: characterization of *Escherichia coli* CYaY as an iron donor for the assembly of [2Fe-2S] clusters in the scaffold IscU. *J. Biol. Chem.*, **281**, 16256–16263.
60. Richards, T.A. and van der Giezen, M. (2006) Evolution of the Isd11-IscS complex reveals a single alpha-proteobacterial endosymbiosis for all eukaryotes. *Mol. Biol. Evol.*, **23**, 1341–1344.
61. Schoenfeld, R.A., Napoli, E., Wong, A., Zhan, S., Reutenauer, L., Morin, D., Buckpitt, A.R., Taroni, F., Lonnerdal, B., Ristow, M. *et al.* (2005) Frataxin deficiency alters heme pathway transcripts and decreases mitochondrial heme metabolites in mammalian cells. *Hum. Mol. Genet.*, **14**, 3787–3799.
62. Tan, G., Chen, L.S., Lonnerdal, B., Gellera, C., Taroni, F.A. and Cortopassi, G.A. (2001) Frataxin expression rescues mitochondrial dysfunctions in FRDA cells. *Hum. Mol. Genet.*, **10**, 2099–2107.
63. Wong, A. and Cortopassi, G. (2002) Reproducible quantitative PCR of mitochondrial and nuclear DNA copy number using the LightCycler. *Methods Mol. Biol.*, **197**, 129–137.
64. Elbashir, S.M., Harborth, J., Weber, K. and Tuschl, T. (2002) Analysis of gene function in somatic mammalian cells using small interfering RNAs. *Methods*, **26**, 199–213.
65. Fish, W.W. (1988) Rapid colorimetric micromethod for the quantitation of complexed iron in biological samples. *Methods Enzymol.*, **158**, 357–364.
66. Tong, W.H. and Rouault, T.A. (2006) Functions of mitochondrial ISCU and cytosolic ISCU in mammalian iron–sulfur cluster biogenesis and iron homeostasis. *Cell. Metab.*, **3**, 199–210.